Systematic profiling of *Caenorhabditis elegans* locomotive behaviors reveals additional components in G-protein Gαq signaling

Hui Yu[a,1], Boanerges Aleman-Meza[a,1], Shahla Gharib[b,c,1], Marta K. Labocha[a], Christopher J. Cronin[b,c], Paul W. Sternberg[b,c,2], and Weiwei Zhong[a,2]

[a]Department of Biochemistry and Cell Biology, Rice University, Houston, TX 77005; and [b]Howard Hughes Medical Institute and [c]Biology Division, California Institute of Technology, Pasadena, CA 91125

Contributed by Paul W. Sternberg, June 4, 2013 (sent for review March 8, 2013)

Genetic screens have been widely applied to uncover genetic mechanisms of movement disorders. However, most screens rely on human observations of qualitative differences. Here we demonstrate the application of an automatic imaging system to conduct a quantitative screen for genes regulating the locomotive behavior in *Caenorhabditis elegans*. Two hundred twenty-seven neuronal signaling genes with viable homozygous mutants were selected for this study. We tracked and recorded each animal for 4 min and analyzed over 4,400 animals of 239 genotypes to obtain a quantitative, 10-parameter behavioral profile for each genotype. We discovered 87 genes whose inactivation causes movement defects, including 50 genes that had never been associated with locomotive defects. Computational analysis of the high-content behavioral profiles predicted 370 genetic interactions among these genes. Network partition revealed several functional modules regulating locomotive behaviors, including sensory genes that detect environmental conditions, genes that function in multiple types of excitable cells, and genes in the signaling pathway of the G protein Gαq, a protein that is essential for animal life and behavior. We developed quantitative epistasis analysis methods to analyze the locomotive profiles and validated the prediction of the γ isoform of phospholipase C as a component in the Gαq pathway. These results provided a system-level understanding of how neuronal signaling genes coordinate locomotive behaviors. This study also demonstrated the power of quantitative approaches in genetic studies.

gene network | high-content screening | locomotion

A number of neuronal signaling genes are known to regulate locomotive behaviors of animals. For example, disruption of the heterotrimeric G protein subunit Gαq in neurons caused movement disorders in *Caenorhabditis elegans* and mice (1, 2). The Gαq signaling pathway is composed of proteins and lipids conserved in all animals (3–5). The main target of Gαq is phospholipase C (PLC), which converts phosphatidylinositol 4,5-bisphosphate to the second messengers, diacyl glycerol (DAG) and inositol trisphosphate (3–5). In *C. elegans* excitatory motor neurons, DAG promotes ACh release, necessary for locomotion.

Despite the wealth of information on individual signaling genes and pathways, a system-level understanding remains missing on how these genes coordinate animal behavior. For example, among all neuronal signaling genes, which ones are involved in regulating a specific stereotyped behavior? How do these genes interact with each other to form networks that process information? A successful method to uncover large-scale gene networks in metazoans is high-content phenotypic profiling. Using binary parameters to score presence and absence of multiple phenotypic details, this approach enabled computational approaches such as hierarchical clustering to infer interactions among development genes (6–8). Behavioral phenotypes such as movement disorders are intrinsically quantitative. Therefore, a quantitative method is needed to extend such an approach to examine behavioral gene networks.

A quantitative behavioral study will also extend our knowledge on individual genes and pathways. For example, although numerous genetic screens have been performed on Gαq signaling, most of these screens rely on human observations that limit their scope to qualitative differences. Therefore, our knowledge for Gαq, one of the most studied genes, is limited to major pathway components that have drastic effects. A quantitative screen will thus complement this knowledge by detecting pathway components with subtle phenotypic differences.

Here we demonstrate the application of an automated imaging system, WormTracker (9, 10), to conduct quantitative, high-content profiling of *C. elegans* locomotive behaviors. We systematically analyzed 227 neuronal signaling genes to understand the gene networks regulating locomotive behaviors. We identified 87 genes required for locomotion and predicted 370 interactions among the genes. Our results enabled reconstruction of known interactions with Gαq and discovery of others. In particular, we discovered PLCγ as a component in the Gαq pathway that functions in parallel to the known Gαq target, PLCβ. Our data are publicly available at www.WormLoco.org.

Results

Phenotypic Profiling of *C. elegans* Locomotive Behaviors. The WormTracker consists of a digital camera, a microscope with a motorized stage, and a computer controlling the camera and the stage (Fig. 1*A*). It tracks a worm by automatically recentering the animal when it reaches the border of the field of view. This system records a high-resolution video of the animal, reduces the animal to 13 equally distributed points along the midline, and quantitatively measures multiple parameters of the sinusoidal movement of *C. elegans* (9, 10).

Among all signaling genes with neuronal expression in *C. elegans*, 227 genes have viable homozygous mutants publicly available (WormBase version WS220). These genes encode a broad spectrum of proteins including neuropeptides, neurotransmitter receptors, and protein kinases (Table S1). We obtained 239 loss-of-function alleles of these genes and used the WormTracker to record each animal for 4 min. We examined at least 10 animals for each genotype and analyzed over 4,400 animals.

The WormTracker measures a total of 66 *C. elegans* locomotive parameters (Table S2). We chose 10 representative parameters that are independent of each other and showed low variance among wild-type animals (*SI Results* and Tables S3 and S4). The parameters are velocity, flex, frequency, amplitude,

Author contributions: H.Y., B.A.-M., P.W.S., and W.Z. designed research; H.Y., B.A.-M., S.G., and W.Z. performed research; C.J.C. contributed new reagents/analytic tools; B.A.-M., M.K.L., and W.Z. analyzed data; and P.W.S. and W.Z. wrote the paper.

The authors declare no conflict of interest.

[1]H.Y., B.A.-M., and S.G. contributed equally to this work.

[2]To whom correspondence may be addressed. E-mail: pws@caltech.edu or weiwei.zhong@rice.edu.

This article contains supporting information online at www.pnas.org/lookup/suppl/doi:10.1073/pnas.1310468110/-/DCSupplemental.

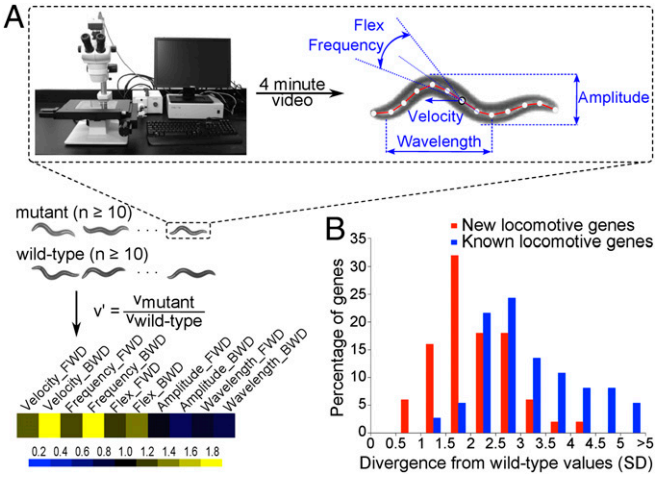

Fig. 1. A quantitative, high-resolution assay to measure *C. elegans* locomotion. (*A*) Experimental pipeline. Each animal was placed on the WormTracker and recorded for 4 min. The video was analyzed to measure several parameters. Parameters measured during forward (FWD) and backward (BWD) movements were analyzed separately. The average values of the mutant group were then normalized by the average of wild-type (N2) data to compose the behavioral profile for this genotype. On the heat map, each cell represents the normalized value of a parameter. Yellow, higher than wild-type; blue, lower than wild-type. The same color scale is used in all figures. (*B*) Histogram of z-scores, showing that this locomotive assay is highly sensitive.

and wavelength for both forward and backward locomotion. They measure the speed of the animal, the propagation of the sinusoidal wave along the axis of the worm body, and the shape of the wave (Fig. 1*A*).

Because the parameters are measured in different units, a normalization process is needed to facilitate further analysis. We used wild-type animals tracked on the same day as controls. The parameter values of mutants were divided by the means of control values to obtain a normalized dataset, so that 1 is the wild-type value for each parameter (Fig. 1*A*). This process also normalized day-to-day environmental variance. Overall, our data collection step produced a quantitative, multiparameter behavioral profile for each of the mutants.

Neuronal Signaling Genes Required for Locomotive Behaviors. Among the 239 mutants we analyzed, 119 mutants of 111 genes displayed abnormality in their locomotive behaviors with at least one parameter significantly different from wild-type values ($P < 0.0001$, Student t test). Among these, 36 strains were unoutcrossed. To verify whether the phenotypes of these mutants were due to background mutations, we performed RNAi of these 36 genes on the strain TU3401, a strain that is sensitized to RNAi in neurons and desensitized to RNAi in other tissues (11). TU3401 animals showed no significant locomotive phenotype. We evaluated RNAi phenotypes by comparing TU3401 animals on RNAi bacteria with those on control bacteria. Twelve genes displayed RNAi phenotypes consistent with those of mutants (*SI Results*). Most of the remaining RNAi did not show any apparent locomotive phenotype, possibly owing to low RNAi penetrance. After the genetic screen and RNAi verification process (Tables S5 and S6), we identified 87 neuronal signaling genes involved in regulating locomotive behaviors.

Eighty of these 87 locomotive genes have mammalian orthologs, including 37 genes that have implications in human diseases (Table S7). Among the 87 locomotive genes, 50 (57%) have never been associated with locomotive phenotypes (WormBase WS220). The mean mutant parameter values from 27 (54%) of these 50 genes are within 2 SD (z-score of 2) shifts from wild-type values (Fig. 1*B*). In contrast, only three (8%) of the previously known locomotive genes have mutant phenotypes in this subtle range (Fig. 1*B*). These data strongly demonstrated that our quantitative approach is highly sensitive in detecting movement disorder genes, particularly those with subtle phenotypes.

Gene Networks Regulating Locomotive Behaviors. To obtain a systematic view of the locomotive gene network, we computed the absolute value of the Pearson correlation coefficient (|PCC|) for each pair of genes to capture genes with similar and opposite behavioral profiles. A |PCC| value of 0 indicates no correlation between two profiles, and 1 indicates a perfect correlation. Among the 87 locomotive genes, there are 54 known genetic interactions (WormBase WS220). Compared with all 3,741 possible pairs among the 87 genes, the majority of these interacting gene pairs have |PCC| above 0.7 (67% vs. 42%, Fig. 2*A*). This suggested that |PCC| is an effective predictor for genetic interactions. Using |PCC| of 0.7 as a threshold, we obtained 1,574 probable interactions among the locomotive genes.

To further prioritize these probable interactions, we queried www.GeneOrienteer.org, a database that integrates cross-species functional data to predict genetic interactions (12). GeneOrienteer examines each *C. elegans* gene pair and its orthologous pairs in eight eukaryote species for features such as physical or genetic interactions, identical expression pattern, related phenotypes, and similar gene ontology annotations. Each feature is assigned a weighted score, and the combined score of all features indicates the likelihood of an interaction. Known interacting locomotive genes are enriched with high GeneOrienteer scores (Fig. 2*A*), indicating that GeneOrienteer scores are another good predictor for genetic interactions. GeneOrienteer predicted 762 interactions (score >4) among the locomotive genes. Three hundred seventy of these pairs also have |PCC| above 0.7, forming a group of high-confidence interactions. Ninety-three percent (344/370) of these high-confidence interactions have not previously been reported.

Sixty-eight of the 87 locomotive genes are connected by the 370 high-confidence predicted interactions. We used the graph partition software METIS (13) to automatically split the genes into five groups based on their connectivity (Fig. 2*B*). Surprisingly, these groups revealed several distinct classes of locomotive genes. One group (green in Fig. 2*B*) is enriched with genes that are involved in response to environmental changes. For example, 7 of 14 of these genes (*daf-11*, *daf-19*, *egl-2*, *inx-4*, *inx-19*, *tax-2*, and *tax-6*) are expressed in sensory neurons and required for normal chemotaxis (WormBase W220). Three other genes in this group (*tpa-1*, *daf-1*, and *chn-1*) are known to regulate feeding and growth/dauer formation (WormBase W220). Another group of 12 genes (blue in Fig. 2*B*) function in other excitable cells such as muscle and intestine to regulate rhythmic movements such as pharyngeal pumping and defecation. Eight genes in this group (*aex-3*, *dyb-1*, *dys-1*, *eat-2*, *gpb-2*, *itr-1*, *rap-1*, and *unc-44*) are expressed in muscle or intestine cells in addition to neurons. Five genes (*aex-3*, *dgk-1*, *eat-2*, *gpb-2*, and *itr-1*) are known to regulate pharyngeal pumping or defecation. As key regulators of locomotive behavior, components in the EGL-30/Gαq signaling network (*eat-16*, *egl-30*, *egl-8*, *unc-73*, *egl-10*, and *goa-1*) span two groups (pink and purple in Fig. 2*B*), suggesting diverse functions of this class. We did not detect a consensus of gene function for only one group of genes (yellow in Fig. 2*B*).

Predicted Gαq Subnetwork. As an example of these high-confidence interactions, we examined the predicted interactions for Gαq. In *C. elegans*, Gαq is encoded by the gene *egl-30*. As illustrated in Fig. 3*A*, EGL-30/Gαq is known to directly act on EGL-8, a β isoform of PLC, to produce DAG in motor neurons (3, 4). EGL-8 was argued not to be the only effector of EGL-30/Gαq because *egl-30* null mutants arrest as larvae whereas *egl-8* null mutants are viable (14). A later study argued that the Rho GEF domain of UNC-73/Trio (referred to as UNC-73 hereafter) was the other EGL-30/Gαq target (15). It was suggested that

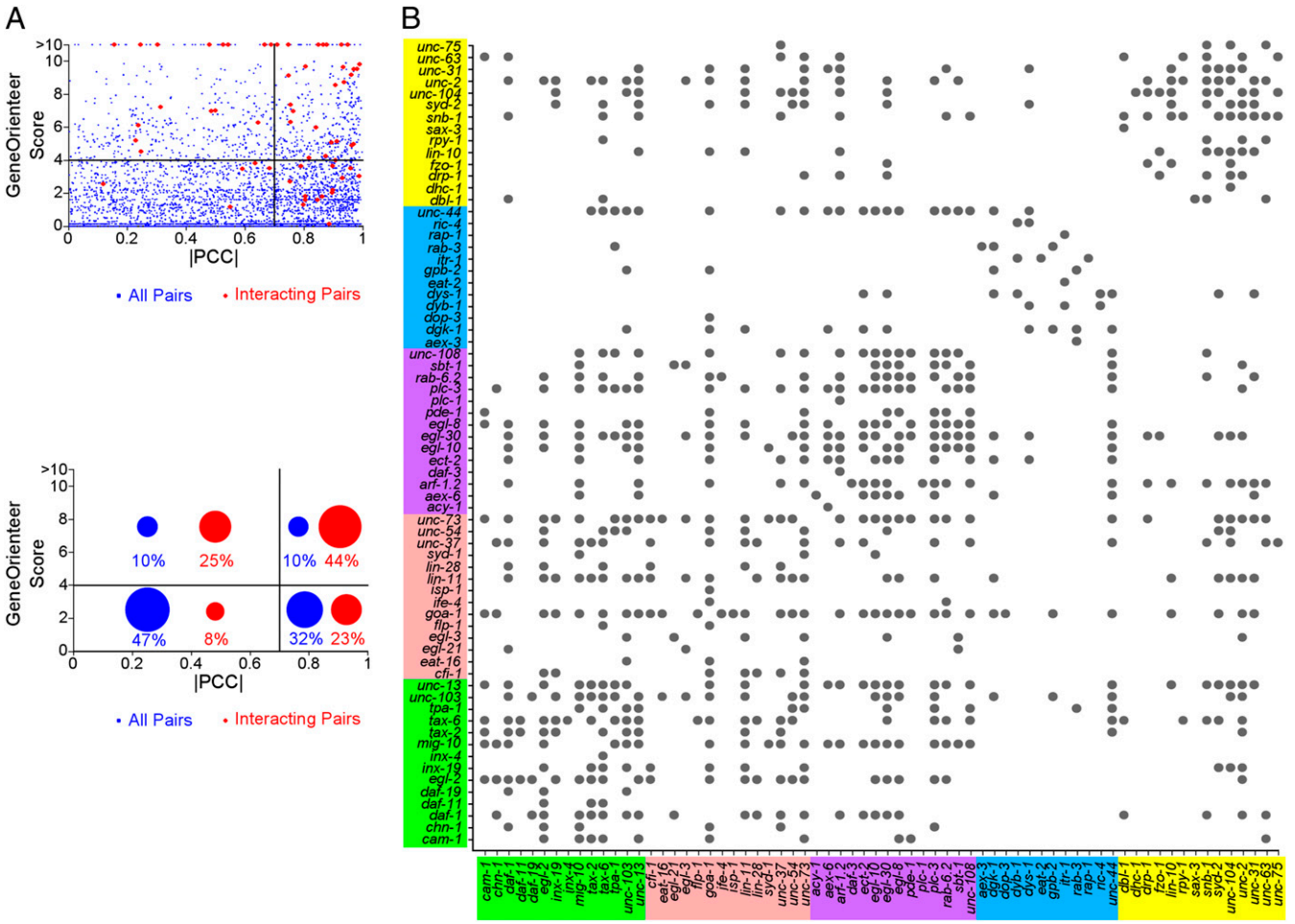

Fig. 2. Predicted genetic interactions among locomotive genes. (*A*) Distribution of |PCC| values and GeneOrienteer scores: interacting genes have higher |PCC| values and GeneOrienteer scores. (*Upper*) A scatterplot with each dot representing a gene pair. (*Lower*) Percentage of gene pairs in each quadrant. (*B*) Predicted network of locomotive genes. Genes in different partitions of the graph are labeled in different colors. A dot indicates a predicted interaction.

UNC-73 functions in parallel or downstream of the DAG kinase DGK-1 and inhibits the conversion of DAG to phosphatidic acid (16, 17). Although this explains how UNC-73 stabilizes DAG once it is produced, it remains unclear how UNC-73 regulates the production of DAG. With EGL-8 being the only known DAG producer, we still cannot explain the phenotypic differences between *egl-8* and *egl-30* null mutants.

Our list of high-confidence interactions suggested 30 genes as *egl-30* interaction candidates, including seven genes known to function in the *egl-30* pathway (Fig. 3*B*). These 30 genes and *egl-30* form a densely connected subnetwork with 219 high-confidence interactions. Among the most connected genes in this subnetwork is *plc-3* (Fig. 3*B*), a gene that has not been previously associated with *egl-30*. Further, *plc-3* was partitioned into the same group with *egl-30* (Fig. 2*B*), suggesting a close association of *plc-3* and *egl-30*. *plc-3* encodes the γ isoform of PLC. This sparks an exciting hypothesis that PLC-3 is the missing PLC in the EGL-30/Gαq pathway that functions in the UNC-73 branch in parallel to EGL-8 to catalyze DAG production (Fig. 3*A*).

PLCγ Functions in the Gαq Signaling Pathway. To test the hypothesis that PLC-3/PLCγ and EGL-8/PLCβ are two EGL-30/Gαq targets, we examined the double mutant lacking both *egl-8* and *plc-3*. If the hypothesis is true, the double mutant should have the larval arrest phenotype resembling that of *egl-30* null alleles. This is exactly what we observed. Whereas null alleles of either *plc-3* or *egl-8* showed no apparent larval arrest, the double mutant *plc-3*(*tm1340*);*egl-8*(*n488*) displayed complete larval arrest (Fig. 3*C*). In contrast, double mutants of *unc-73* and *plc-3* displayed no synthetic effect. Is the larval lethality of *plc-3*(*tm1340*);*egl-8*(*n488*) similar to that of *egl-30* null mutants? Phorbol 12-myristate 13-acetate (PMA), a DAG analog, can rescue the larval arrest phenotype of *egl-30* null mutants (18). If EGL-30 acts through PLC-3 and EGL-8 to produce DAG, then PMA should also rescue the larval arrest phenotype of *plc-3*(*tm1340*);*egl-8*(*n488*) double mutants. Indeed, the double mutant showed a developmental profile similar to that of wild-type animals when exposed to PMA (Fig. 3*D*). In the control group, when the animals were cultured on the PMA solvent ethanol, all *plc-3* (*tm1340*);*egl-8*(*n488*) animals were young larvae when wild-type animals became adults (Fig. 3*D*). Therefore, *egl-8* and *plc-3* likely function in parallel as *egl-30* targets. It has been reported that the Double mutants of *egl-8* and *unc-73* also displayed synthetic larval lethality that can be rescued by PMA (15). Such phenotypic similarity between *plc-3* and *unc-73* is consistent with our model that *plc-3* functions in the *unc-73* branch parallel to *egl-8*.

In the *C. elegans* genome, there are five PLCs in four isozyme families: PLC-2 and EGL-8 (PLCβ), PLC-3 (PLCγ), PLC-4(PLCδ), and PLC-1(PLCε). We then asked whether the interaction between EGL-8 and PLC-3 is a specific interaction or a general redundancy among all PLCs. To answer this, we examined null alleles of all PLCs for their locomotion behavior (Fig. 3*E*). Besides *egl-8* and *plc-3*, only *plc-1* displayed locomotive phenotypes ($P < 0.0001$ for at least one parameter). However, in contrast to

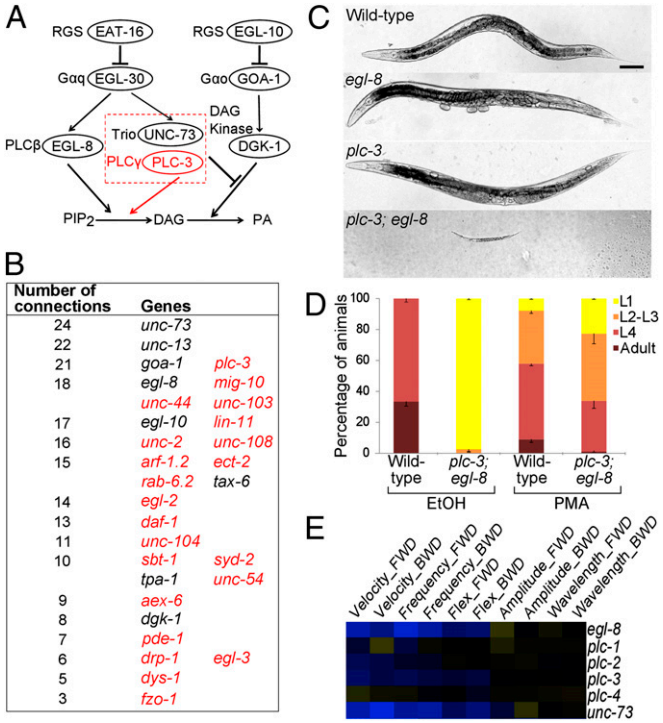

Fig. 3. PLC-3 is the missing PLC in the EGL-30 network. (*A*) Simplified model of EGL-30 effectors. Black, known interaction; red, proposed interaction. (*B*) Genes and number of connections in the predicted EGL-30/Gαq network. Black, known components in the EGL-30/Gαq network; red, predicted components. (*C*) Null mutations for EGL-8 and PLC-3 have a synthetic larval arrest phenotype. All images were captured using the same scale. (Scale bar, 100 μm.) (*D*) Developmental profiles of animals exposed to either ethanol (EtOH) or PMA in ethanol, showing that PMA rescues the larval arrest of *egl-8* and *plc-3* double-null mutants. Data are means and SE of three trials with 50 animals in each trial. (*E*) Behavioral profiles of mutants for two known EGL-30 targets (EGL-8 and UNC-73) and all PLCs.

the *plc-3* behavioral profile, which is highly similar to that of *egl-8* and *unc-73* (PCC of 0.94 and 0.94, respectively), the *plc-1* profile showed little similarity to those two known *egl-30* targets (PCC 0.53 and 0.32). The double mutant of *plc-1* and *egl-8* also did not display any synthetic larval arrest. Therefore, the interaction between *egl-8* and *plc-3* is highly specific.

Epistasis Analysis of Behavioral Profiles with Opposite Phenotypes. A powerful method to infer genetic interactions is epistasis analysis. Epistasis analysis places genes in pathways by comparing double mutant phenotypes to those of single mutants. However, classical epistasis analysis does not readily accommodate our quantitative, multiparameter data. Inspired by the concept of quantitative epistasis analysis applied to yeast metabolic networks and slime mold expression data (19, 20), we sought a new strategy to extract epistasis from the behavioral profiles such as those listed in Fig. 4*A*. The method should reconstruct known epistatic relationships as well as identify new ones such as the model of PLC-3 function in the EGL-30 pathway.

One principle of epistasis analysis is that if two genes with contrasting phenotypes function in a linear pathway, then the double mutant shows the phenotype of the downstream gene. We selected two groups of genes with opposite functions from the EGL-30/Gαq network to test whether we can reconstruct known interactions solely based on behavioral profiles. In one group are EAT-16 and DGK-1, both of which suppress ACh release. In the other group are EGL-10 and EGL-30, both of which promote ACh release. Accordingly, mutants of genes with identical functions displayed similar (positively correlated) locomotive phenotypes, whereas mutants of genes with opposite functions displayed contrasting (negatively correlated) locomotive phenotypes (Fig. 4*B*). Correlations of phenotypic patterns are, however, not suitable for epistasis analysis because they do not capture phenotype severity. For example, the behavioral profiles showed that *eat-16* and *egl-10* single mutants have drastically contrasting phenotypes, and that their double mutant has an almost wild-type behavioral profile (Fig. 4*A*). The additive effects of these two genes on the double mutant suggested that these two genes function in parallel. However, the PCC method misaligned *egl-10* to be downstream of *eat-16* because the double mutant is positively correlated to *egl-10* and negatively correlated to *eat-16* (Fig. 4*C*).

It is known that the EAT-16 protein directly inhibits EGL-30, and *dgk-1* mutations are epistatic to *egl-10* (4). To reconstruct such epistatic relationships from our locomotive data, we used the Manhattan distance to quantify the similarity between behavioral profiles. Given two phenotypic profiles A and B with parameter values (A_1, A_2,… A_n) and (B_1, B_2,… B_n), their Manhattan distance is defined as $d(A,B) = \sum_{i=1}^{n} |A_i - B_i|$. We designated the single mutant with longer distance to the double mutant as "upstream" and the less divergent single mutant as "downstream." If we set the distance between the double and the upstream mutant as 1, then the normalized distance between the double and the downstream mutant (d_{down}) is a value between 0 and 1. The d_{down} value should be close to 0 if the two genes function in a linear pathway and close to 1 otherwise. We reasoned that a linear relationship is strongly suggested by an upstream distance more than five times the magnitude of the downstream distance, corresponding to d_{down} <0.2. Using d_{down} = 0.2 as a cutoff for linear relationship, we carried out the analysis on the locomotive profiles and successfully reconstructed the known relationships of *egl-30* being downstream of *eat-16*, and *dgk-1* being downstream of *egl-10* (Fig. 4*D*). We also found that neither *egl-8* nor *plc-3* showed a linear epistatic relationship to

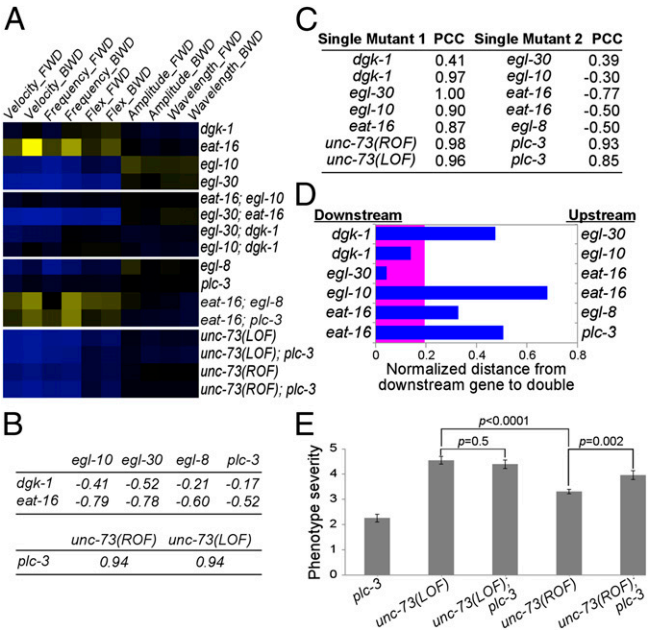

Fig. 4. Quantitative epistasis analysis of EGL-30/Gαq network components. (*A*) Behavioral profiles of single and double mutants. (*B*) PCC of behavioral profiles with opposite or similar phenotypes. (*C*) PCC of behavioral profiles of each double mutant and its corresponding two single mutants. (*D*) Normalized distance between double mutants and corresponding downstream gene mutants (d_{down}). Pink area marks d_{down} ≤0.2, where two genes are considered epistatic. (*E*) Phenotype severity of single and double mutants. LOF, loss of function; ROF, reduction of function. Data are means and SE. *P* values are calculated using Student *t* test.

eat-16 (Fig. 4*D*), which is consistent with our model that *plc-3* and *egl-8* are two branched targets of *egl-30* (Fig. 3*A*).

Epistasis Analysis of Behavioral Profiles with Similar Phenotypes. The principle of epistasis analysis for two genes with similar phenotypes is that if two genes function in the same pathway, the double null mutant phenotype should be no more severe than that of the single null mutants. We applied this to examine whether *plc-3* functions with *unc-73* in the same pathway. *plc-3* and *unc-73* have highly similar phenotypes (Fig. 4*B*). To quantify phenotype severity, we computed the distance between a mutant and wild-type (*wt*) profiles. For example, the phenotype severity of a mutant profile (A_1, A_2,... A_n) is $d(A, wt) = \sum_{i=1}^{n} |A_i - 1|$. Our data showed that *unc-73*(*ev802*), a null loss-of-function allele of the Rho GEF domain, has a more severe locomotion phenotype than *unc-73*(*ce362*), a nonnull reduction-of-function allele (Fig. 4E), validating the sensitivity of our assay in detecting phenotypic differences. A *plc-3* null allele, *plc-3*(*tm1340*), enhanced the phenotype severity of *unc-73*(*ce362*) but not *unc-73*(*ev802*) (Fig. 4*E*), suggesting that *plc-3* and *unc-73* function in the same pathway.

Open-Access Data Resource. All our data, including over 300 h of video, 66 parameter measurements for each animal, and statistics for each experimental group, are publicly available at www.WormLoco.org. In addition, one can also query and download similar or opposite phenotypic patterns and predicted interaction scores.

Discussion

Quantitative Profiling of Locomotive Behaviors. Compared with classic genetic screens, our quantitative approach showed several advantages. It is more sensitive in detecting subtle phenotypes, enabling us to discover more genes regulating motor behavior. In addition, it provides higher data content with multiple parameters, allowing us to conduct bioinformatic analysis to deduct the interaction network of these signaling genes. Finally, combined with a large number of animals surveyed, it provides insights on the intrinsic nature (e.g., variation and dependency) of phenotypic parameters.

Our results revealed that genetic screens are far from saturation in exploring locomotive defects, particularly in the quantitative domain. We were able to discover 50 additional neuronal signaling genes that affect locomotion and 23 additional components in the extensively studied Gαq network. When we visually examined mutants of those genes, we were unable to detect any locomotive phenotype in many mutants including *plc-3*. The WormTracker or similar imaging systems are crucial for capturing those subtle phenotypes.

Several imaging systems have been developed for animal behavior analysis. A low-resolution approach reduces the animal to one point and analyzes velocity and other position-based parameters (21, 22). This method is efficient for simultaneous recording of multiple animals. The WormTracker took a different approach and used a high resolution to represent a worm with 13 points. This enabled measurement of parameters such as body shape. However, the high-resolution approach also limits the throughput to one animal at a time. Therefore, we used a short recording time (4 min) to accommodate a large-scale screen. This short recording time makes our analysis focused on acute locomotive defects. A longer recording time will enable analysis of other phenotypes such as sleep/awake patterns.

Whereas 10 parameters were used in this study, our data can be used to derive more locomotive parameters. For example, we can normalize wavelength and amplitude by body length. Further, animal-to-animal variation of some parameters can also provide new measurements (*SI Results*). In addition to the 66 locomotive parameters measured in this analysis, the WormTracker can be programmed to measure more complicated patterns of behaviors (23).

Neuronal Signaling Gene Network. A major challenge in studying signaling genes is to identify how these genes interact (Fig. S1). Although epistasis analysis provides direct experimental evidence of genetic interactions, this method requires inactivation of two genes. Constructing double mutants in metazoans is a low-throughput process, and *C. elegans* neuronal genes are resistant to feeding RNAi, unless in a sensitized genetic background (24), therefore, computational predictions became a more practical method to map neuronal signaling gene networks by prioritizing experiments.

By integrating the behavioral profiles, we obtained experimentally and publicly available functional data and we predicted 370 interactions among 68 genes. Partition of this network based solely on connectivity revealed several interesting functional modules regulating locomotion. In addition to the well-established Gαq signaling modules, we found two additional classes of genes modulating locomotive behaviors. The first is a class of genes functioning in sensory neurons, presumably coordinating locomotive behavior with environmental changes. The second is a class of genes that function in muscles or intestine cells in addition to neurons. These genes are likely required for basic functions of excitable cells.

PLC-3 as an EGL-30/Gαq Target. The finding of PLC-3 as an additional EGL-30/Gαq target strongly demonstrated the power of our quantitative approach. The EGL-30/Gαq pathway has been studied extensively for decades for its role in regulating locomotion and egg-laying behavior, and has been long hypothesized to have a missing PLC in addition to EGL-8/PLCβ (see refs. 3 and 4 for reviews). *plc-3* has likely escaped detection in numerous locomotion-based screens because its locomotion defects are too subtle to be detected by human observation. *plc-3* also eluded detection in chemical screens (*SI Results* and Fig. S2) or screens for abnormal egg-laying because of its other phenotypes such as sterility.

Among the five PLCs in the *C. elegans* genome, PLC-3 and EGL-8 may share similar functions in more than one biological process. Consistent with our observation of PLC-3 and EGL-8 functioning together in regulating locomotive behaviors and larval development, it was reported that both PLC-3 and EGL-8 share functional redundancy with PLC-1 in embryogenesis (25), and that PLC-3 and EGL-8 function in parallel to regulate rhythmic Ca^{2+} oscillations in the intestine (26). Because PLCs are highly pleiotropic, it is possible that PLC-3 and EGL-8 may function together in multiple traits.

There is no systematic study on *plc-3* expression pattern. Therefore, we cannot pinpoint the PLC-3 site of action. It was reported that UNC-73 has EGL-30–independent functions regulating locomotive behaviors in neurons other than motor neurons (17). It would be interesting to find whether PLC-3 also functions in those cells.

Quantitative Epistasis. We developed unique quantitative epistasis analysis methods to extract genetic interactions from these behavioral profiles. Such methods can be extended beyond genetic screens. For example, automatic behavioral profiling enabled a screen of over 5,000 psychoactive drugs for chemicals affecting zebrafish sleep/awake patterns (22). Our method of quantitative epistasis analysis might be applicable to discover gene–drug or drug–drug interactions. This study provides a framework to further explore the potential of such high-throughput, quantitative approaches in addressing basic biological questions.

Methods

Animal Culture. *C. elegans* strains were cultured on Nematode Growth Medium at 20 °C as described (27, 28). Bristol N2 was used as the wild-type strain.

Strains. The strains we tested are listed in Table S1. We obtained gene expression data from WormBase (version WS220) to find neuronally expressed genes, gene function annotation from Gene Ontology to find

cell signaling genes, and strain information from the Caenorhabditis Genetics Center (CGC) to find viable homozygous mutants. We selected mutants from the intersection of the three datasets and obtained them from the CGC.

When there were multiple alleles for a gene, we chose the allele based on the following criteria (ranked in preference):

(*i*) An allele that is well documented and has been referenced by multiple publications;
(*ii*) An allele that has been well characterized and sequenced;
(*iii*) A null allele with a stop codon or a deletion mutant;
(*iv*) A strain that has been outcrossed; and
(*v*) A mutant with a simple genetic background and no secondary mutations in other genes. We avoided mutants with a high Tc1 copy number.

The RNAi-sensitized strain TU3401 [*sid-1*(*pk3321*) *V; uIs69 V*] (11) was used in RNAi experiments. The genotype for *uIs69* is [*pCFJ90*(*myo-2p::mCherry*) + *unc-119p::sid-1*].

The following alleles were used for the epistasis analysis in Fig. 4: *egl-8* (*n488*) (the canonical null allele, or a possible neomorphic allele that better represents the null phenotype than other alleles in behavioral assays) (14), *egl-30*(*ad809*) (the strongest viable allele) (1), *dgk-1*(*sy428*) (a putative null allele) (29, 30), *eat-16*(*sy438*) (a putative null allele) (29), *plc-3*(*tm1340*) (a null allele), *unc-73*(*ev802*) [a Rho guanine nucleotide exchange factor (GEF) domain null allele] (31), *unc-73*(*ce362*) (a strong reduction of function allele for the Rho GEF activity) (15). Although *egl-30*(*ad809*) is not a null allele, its locomotive phenotypes are stronger than those of *egl-8*(*n488*) (distance to wild-type 4.52 ± 0.13 vs. 3.25 ± 0.11, respectively, $P < 0.001$, Student *t* test). This was consistent with the knowledge that *egl-8* is not the only target of *egl-30* (15) and suggested that the *egl-30* allele is strong enough for epistasis analysis of locomotive behaviors.

Worm Tracking. We applied the WormTracker to track *C. elegans* locomotion following a protocol described previously (9) (*SI Methods*). First-day adult animals were analyzed on a fresh bacterial lawn at 20 °C.

RNAi. RNAi was performed as described (32, 33) (*SI Methods*). Animals at larval stage L4 were placed on RNAi bacteria and cultured at 20 °C. Their progeny were analyzed at the stage of first-day adults.

Phorbol Ester Rescue Experiment. PMA (5 μM) was administered as described (18, 34) (*SI Methods*).

ACKNOWLEDGMENTS. We thank the Caenorhabditis Genetics Center (CGC), Erin Cram, and Shohei Mitani for strains, Illya Hicks for helpful discussions, Joaquina Nunez, Barbara Perry, and Julie Nguyen for technical assistance, Ranjana Kishore for a critical reading of the manuscript, and WormBase. This work was supported by National Institutes of Health Grant HG004724 and a Searle Scholar grant from the Kinship Foundation (to W.Z.), by National Institutes of Health Grant DA018341 (to P.W.S. and W.Z.), and by the Howard Hughes Medical Institute, with which P.W.S. is an investigator. CGC is funded by National Institutes of Health Office of Research Infrastructure Programs Grant P40 OD010440.

1. Brundage L, et al. (1996) Mutations in a C. elegans Gqalpha gene disrupt movement, egg laying, and viability. *Neuron* 16(5):999–1009.
2. Hartmann J, et al. (2004) Distinct roles of Galpha(q) and Galpha11 for Purkinje cell signaling and motor behavior. *J Neurosci* 24(22):5119–5130.
3. Perez-Mansilla B, Nurrish S (2009) A network of G-protein signaling pathways control neuronal activity in C. elegans. *Adv Genet* 65:145–192.
4. Bastiani C, Mendel J (2006) Heterotrimeric G proteins in C. elegans. *WormBook* 2006: 1–25.
5. Wettschureck N, Offermanns S (2005) Mammalian G proteins and their cell type specific functions. *Physiol Rev* 85(4):1159–1204.
6. Green RA, et al. (2011) A high-resolution C. elegans essential gene network based on phenotypic profiling of a complex tissue. *Cell* 145(3):470–482.
7. Gunsalus KC, et al. (2005) Predictive models of molecular machines involved in Caenorhabditis elegans early embryogenesis. *Nature* 436(7052):861–865.
8. Sönnichsen B, et al. (2005) Full-genome RNAi profiling of early embryogenesis in Caenorhabditis elegans. *Nature* 434(7032):462–469.
9. Cronin CJ, et al. (2005) An automated system for measuring parameters of nematode sinusoidal movement. *BMC Genet* 6:5–23.
10. Feng ZY, Cronin CJ, Wittig JH, Jr., Sternberg PW, Schafer WR (2004) An imaging system for standardized quantitative analysis of C. elegans behavior. *BMC Bioinformatics* 5:115.
11. Calixto A, Chelur D, Topalidou I, Chen X, Chalfie M (2010) Enhanced neuronal RNAi in C. elegans using SID-1. *Nat Methods* 7(7):554–559.
12. Zhong W, Sternberg PW (2006) Genome-wide prediction of C. elegans genetic interactions. *Science* 311(5766):1481–1484.
13. Karypis G, Kumar V (1999) A fast and high quality multilevel scheme for partitioning irregular graphs. *SIAM J Sci Comput* 20(1):359–399.
14. Bastiani CA, Gharib S, Simon MI, Sternberg PW (2003) Caenorhabditis elegans Galphaq regulates egg-laying behavior via a PLCbeta-independent and serotonin-dependent signaling pathway and likely functions both in the nervous system and in muscle. *Genetics* 165(4):1805–1822.
15. Williams SL, et al. (2007) Trio's Rho-specific GEF domain is the missing Galpha q effector in C. elegans. *Genes Dev* 21(21):2731–2746.
16. McMullan R, Hiley E, Morrison P, Nurrish SJ (2006) Rho is a presynaptic activator of neurotransmitter release at pre-existing synapses in C. elegans. *Genes Dev* 20(1): 65–76.
17. Hu S, Pawson T, Steven RM (2011) UNC-73/trio RhoGEF-2 activity modulates Caenorhabditis elegans motility through changes in neurotransmitter signaling upstream of the GSA-1/Galphas pathway. *Genetics* 189(1):137–151.
18. Reynolds NK, Schade MA, Miller KG (2005) Convergent, RIC-8-dependent Galpha signaling pathways in the Caenorhabditis elegans synaptic signaling network. *Genetics* 169(2):651–670.
19. Van Driessche N, et al. (2005) Epistasis analysis with global transcriptional phenotypes. *Nat Genet* 37(5):471–477.
20. Segrè D, Deluna A, Church GM, Kishony R (2005) Modular epistasis in yeast metabolism. *Nat Genet* 37(1):77–83.
21. Kumar V, et al. (2011) Second-generation high-throughput forward genetic screen in mice to isolate subtle behavioral mutants. *Proc Natl Acad Sci USA* 108(Suppl 3): 15557–15564.
22. Rihel J, et al. (2010) Zebrafish behavioral profiling links drugs to biological targets and rest/wake regulation. *Science* 327(5963):348–351.
23. Brown AE, Yemini EI, Grundy LJ, Jucikas T, Schafer WR (2013) A dictionary of behavioral motifs reveals clusters of genes affecting Caenorhabditis elegans locomotion. *Proc Natl Acad Sci USA* 110(2):791–796.
24. Timmons L, Court DL, Fire A (2001) Ingestion of bacterially expressed dsRNAs can produce specific and potent genetic interference in Caenorhabditis elegans. *Gene* 263(1-2):103–112.
25. Vázquez-Manrique RP, et al. (2008) Phospholipase C-epsilon regulates epidermal morphogenesis in Caenorhabditis elegans. *PLoS Genet* 4(3):e1000043.
26. Espelt MV, Estevez AY, Yin X, Strange K (2005) Oscillatory Ca2+ signaling in the isolated Caenorhabditis elegans intestine: Role of the inositol-1,4,5-trisphosphate receptor and phospholipases C beta and gamma. *J Gen Physiol* 126(4):379–392.
27. Brenner S (1974) The genetics of Caenorhabditis elegans. *Genetics* 77(1):71–94.
28. Stiernagle T (2006) Maintenance of C. elegans. *WormBook* 2006:1–11.
29. Hajdu-Cronin YM, Chen WJ, Patikoglou G, Koelle MR, Sternberg PW (1999) Antagonism between G(o)alpha and G(q)alpha in Caenorhabditis elegans: The RGS protein EAT-16 is necessary for G(o)alpha signaling and regulates G(q)alpha activity. *Genes Dev* 13(14):1780–1793.
30. Miller KG, Emerson MD, Rand JB (1999) Goalpha and diacylglycerol kinase negatively regulate the Gqalpha pathway in C. elegans. *Neuron* 24(2):323–333.
31. Steven R, Zhang L, Culotti J, Pawson T (2005) The UNC-73/Trio RhoGEF-2 domain is required in separate isoforms for the regulation of pharynx pumping and normal neurotransmission in C. elegans. *Genes Dev* 19(17):2016–2029.
32. Kamath RS, et al. (2003) Systematic functional analysis of the Caenorhabditis elegans genome using RNAi. *Nature* 421(6920):231–237.
33. Rual JF, et al. (2004) Toward improving Caenorhabditis elegans phenome mapping with an ORFeome-based RNAi library. *Genome Res* 14(10B):2162–2168.
34. Schade MA, Reynolds NK, Dollins CM, Miller KG (2005) Mutations that rescue the paralysis of Caenorhabditis elegans ric-8 (synembryn) mutants activate the G alpha(s) pathway and define a third major branch of the synaptic signaling network. *Genetics* 169(2):631–649.